HEFAT2014
10th International Conference on Heat Transfer, Fluid Mechanics and Thermodynamics
14 – 16 July 2014
Orlando, Florida

TEMPERATURE VARIATION ON THE HEATED BASE OF A SOLID SUBSTRATE COOLED WITH DIFFERENT TYPES OF HEAT SINK

Adewumi O.O[1], Bello-Ochende T[*2] and Meyer J.P[1]
*Author for correspondence
[1]Department of Mechanical and Aeronautical Engineering,
University of Pretoria,
Pretoria 0002,
South Africa.
[2]Department of Mechanical Engineering,
University of Cape Town,
Cape Town,
South Africa.
Email: tunde.bello-ochende@uct.ac.za

ABSTRACT

Three-dimensional numerical studies were carried out to investigate forced convection heat transfer and fluid flow in a solid substrate cooled using different types of micro heat sinks. The objective of this study is to investigate which heat sink type gives the lowest temperature variation on the heated base of the solid substrate which is being cooled. A low temperature variation indicates a low temperature gradient which, in practical application, improves the reliability of the electronic device. The different heat sinks considered are single microchannels, two-layer microchannels with parallel and counter-flow of fluid, single microchannels inserted with circular-shaped micro pin fins and two-layer microchannels inserted with circular-shaped pin fins. All the heat sinks are geometrically optimised using a computational fluid dynamics code with a goal-driven optimisation algorithm subject to global constraints. The thermal performance of the heat sinks considered in this study is based on two objectives namely, the minimisation of the peak temperature which results in maximisation of the thermal conductance and the lowest temperature variation on the heated base. The heat sink with the largest value of thermal conductance and lowest temperature variation on the heated base for the range of pressure drop considered is chosen as the best heat sink design. Numerical results of thermal performance for fixed axial length of the solid showed that cooling the solid substrate with the two-layer microchannel with counter-flow of fluid gave the lowest temperature difference at base of the solid substrate and also performed best in maximising thermal conductance at pressure drops of 20 and 30kPa.

INTRODUCTION

After the pioneering work of Tuckerman and Pease [1] on the removal of high heat fluxes from microelectromechanical systems (MEMS) using single microchannels, numerous investigations have been carried out on the thermal performance of single microchannels [2-12]. The use of stacked microchannels has also been introduced to achieve more effective cooling while maintaining the uniform temperature of the chips because of the larger surface area available for fluid flow [13-15].
In the study carried out by Wei [14], it was observed that for water-cooled silicon microchannels with relatively high aspect ratio, no more than two layers should be stacked since there is no significant benefit in thermal performance beyond two layers while in analytical study carried out by Wei *et al.* [16] where a simple thermal resistance network model was developed and optimisation was carried out using genetic algorithms to minimise the overall thermal resistance of a stacked microchannel heat sink, the optimal number of layers was three for a constant pumping power of 0.01W. Some of the other investigations carried out on multi-layered microchannels are Wei and Joshi [17], Jeevan *et al.* [18, 19], Chong *et al.* [20] and Hung *et al.* [21]. Wei [14] also observed non-uniformity in temperature of the chip being cooled can tremendously affect the reliability and performance of electronic devices. His results showed that the two-layer microchannel with counter flow

arrangement can be applied to reduce chip temperature non-uniformity.

The stacked microchannel design used in the studies outlined above consisted of two or more stacks having the same sizes. This kind of model resulted in increased flow area for the fluid. Recently, a combined design of microchannels and micro pin-fins was modelled and heat transfer through this combined design was numerically investigated by Adewumi *et al.* [22]. Their results showed an improvement in the maximum thermal conductance.

This study is aimed at numerically investigating the temperature variation on the heated base of a solid substrate with different type of heat sink design using a commercially available computational fluid dynamics (CFD) code which a goal-driven algorithm. The heat sink designs considered are single microchannel (single), combined single microchannel and three rows of micro pin fins (ID circular 3 rows), two-layer microchannel with parallel flow of fluid (two-layerPF), two-layer microchannel with counter-flow of fluid (two-layerCF), Combined design of the two-layerPF and three rows of micro pin fins (two-layerPF ID 3 rows) and the combined design of the two-layerCF and three rows of micro pin fins (two-layerCF ID 3 rows). The global objective of this investigation is the maximisation of the thermal conductance which depends on the minimisation of the peak temperature of the solid substrate and also to investigate which heat sink gives the lowest temperature variation on the heated base. Lowering the temperature variation on the heated base minimises the temperature gradient thereby improving the reliability of a microelectronic device.

NOMENCLATURE

A	[m^2]	area
C	[-]	global thermal conductance
C_p	[J/K]	heat capacity
D_f	[m]	diameter of pin fin
$H_{c1,c2}$	[m]	channel height of top and bottom layers
H_f	[m]	pin-fin height
k_s	[W/mK]	thermal conductivity of solid wall
k_f	[W/mK]	thermal conductivity of fluid
M	[m]	height of computational volume
N	[m]	length
P	[Pa]	pressure
q	[W]	heat transfer rate
q''	[W/m^2]	heat flux
T	[^{o}C]	temperature
$t_{1,6}$	[m]	half-width thickness of vertical solid
t_2	[m]	channel base thickness
$t_{3,5}$	[m]	channel base to height distance
u,v,w	[m/s]	velocities in the *x*-, *y*- and *z* directions
V	[m^3]	computational domain volume
W	[m]	computational domain width
$W_{c1,c2}$	[m]	channel width of top and bottom layers
W_t	[m]	total width of solid volume

Special characters

Δ	[-]	difference
ρ	[kg/m^3]	density
μ	[kg/ms]	dynamic viscosity
α	[m^2/s]	thermal diffusivity
ϕ	[-]	volume fraction
Ω	[-]	interface between solid and fluid

Subscripts

atm	atmosphere
f	fluid
max	maximum
min	minimum
opt	optimum
out	outlet
solid	solid
n	number of rows of pin fins
base	heated base

PHYSICAL MODEL

The physical models of all the different heat sinks considered in this study are shown in Figure 1. Figure 1a shows a single microchannel while Figure 1b is a two-layer microchannel heat sink. Figure 1c and 1d show the single and two-layer microchannel with micro pin-fin inserts respectively. Figure 2a and 2b show the parallel and counter-flow arrangements respectively for the two-layer microchannel. The length *N*, height *M* and width *W* of the solid is fixed which makes the volume *V* fixed while t_1, t_2, t_3, t_5, t_6, H_{c1}, H_{c2}, W_{c1} and W_{c2} are varied but also subject to manufacturing constraints.

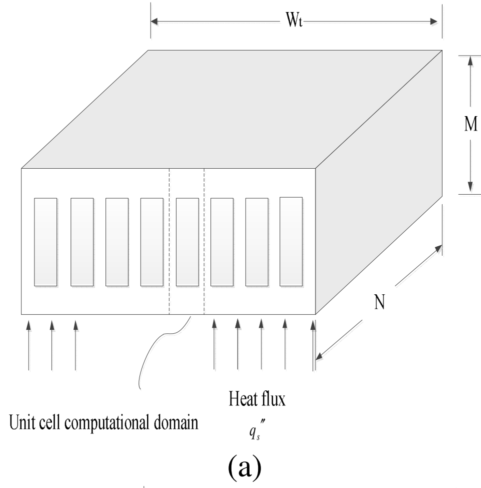

(a)

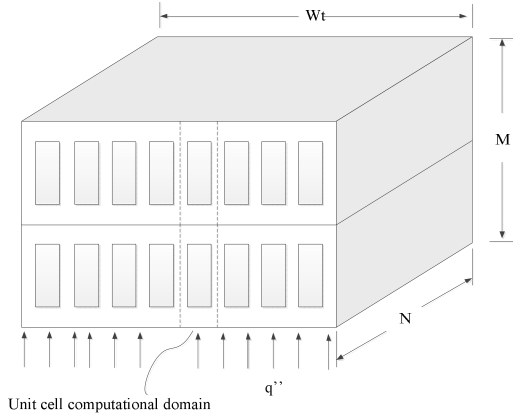

(b)

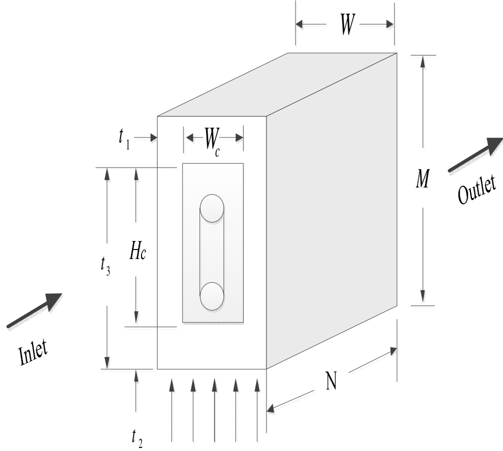

(c)

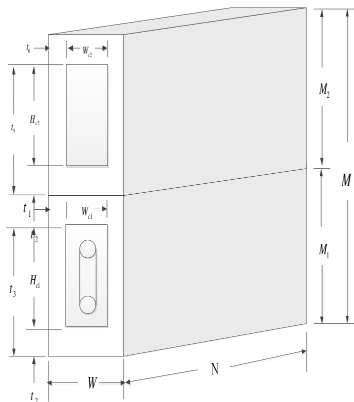

(d)

Figure 1 Different type of heat sinks

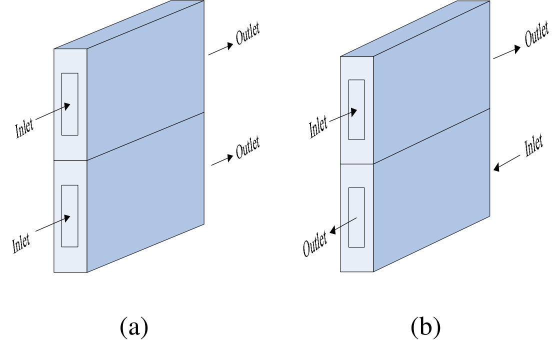

(a) (b)

Figure 2 Different flow arrangements for the two-layer microchannel heat sink

The solid volume fraction or porosity ϕ is defined as the ratio of the solid volume to the total volume of the heat sink which is only dependent on the cross-sectional area of the heat sink as shown in Equation (1).

$$\phi = \frac{V_{solid}}{V} = \frac{A_{solid}N}{AN} = \frac{A_{solid}}{A} = \frac{MW - H_c W_c}{MW} \quad (1)$$

The fixed global volume is defined as

$$V = MWN = const \quad (2)$$

The manufacturing constraints [11, 27] are

$$\frac{H_{c1,c2}}{W_{c1,c2}} \leq 20 \quad (3)$$

$$t_2 \geq 50\mu m \quad (4)$$

$$M - t_3 \geq 50\mu m \text{ (Single-layer)} \quad (5)$$

$$M_2 - t_5 \geq 50\mu m \text{ (Two-layer)} \quad (6)$$

Where

$$M_1 + M_2 = M \quad (7)$$

The micro pin fins inserted in the optimised micro-channel are also subject to the manufacturing constraints [27] in Equations (8) and (9).

$$0.5 \leq \frac{H_f}{D_f} \leq 4.0 \quad (8)$$

$$s \geq 50\mu m \quad (9)$$

A total fin volume constraint is applied to the micro pin fins where the volume of the cylindrical fins is constant.

$$V_f = V_{f1} + V_{f2} + ... + V_{fn} = const \quad (10)$$

GOVERNING EQUATIONS ANDBOUNDARY CONDITIONS

The present study assumes that the flow is steady and laminar. The cooling fluid, which is water, is also assumed to be incompressible with homogeneous and constant thermo-physical properties. The temperature distribution within the geometry used in this study was determined by solving the conservation of mass, momentum and energy Equations (8)-(11) numerically. The governing equations solved after applying the above assumptions are,

$$\nabla \cdot \vec{v} = 0 \quad (11)$$

$$\rho(\vec{v} \cdot \nabla \vec{v}) = -\nabla P + \mu \nabla^2 \vec{v} \quad (12)$$

$$\rho_f C_{pf} (\vec{v} \cdot \nabla T) = k_f \nabla^2 T \quad (13)$$

The energy equation for the solid regions can be written as:

$$k_s \nabla^2 T = 0 \quad (14)$$

The heat flux between the interface of the fluid and the solid walls is coupled and its continuity between the interface of the solid and the liquid is given as:

$$k_s \frac{\partial T}{\partial n}\Big|_\Omega = k_f \frac{\partial T}{\partial n}\Big|_\Omega \quad (15)$$

The inlet boundary conditions are,

$$p = P_{in}, \; v = w = 0 \quad (16)$$

$$T = T_{in} \quad (17)$$

At the outlet, the boundary condition is specified as,

$$P_{out} = P_{atm} \quad (18)$$

Symmetry boundary conditions are specified at the left and right side of the domain,

$$\frac{\partial T}{\partial x} = 0 \quad (19)$$

A no slip boundary condition is specified walls,

$$u = v = w = 0 \quad (20)$$

A constant uniform heat flux q'' is applied at the bottom wall,

$$q'' = k_s \frac{\partial T}{\partial y} \quad (21)$$

The measure of performance is the maximum global thermal conductance, which could be expressed in dimensionless form as

$$C_{max} = \frac{q'' N}{k_f \Delta T} \quad (22)$$

where the excess temperature ΔT is the difference between maximum temperature of the solid substrate and the inlet temperature of the fluid

$$\Delta T = T_{max} - T_{min} \quad (23)$$

While the temperature difference on the heated base of the solid substrate is defined as

$$(\Delta T)_{base} = (T_{max})_{base} - (T_{min})_{base} \quad (24)$$

NUMERICAL PROCEDURE, GRID ANALYSIS AND CODE VALIDATION

The continuity, momentum and energy Equations (11)-(14) along with the boundary conditions (15)-(21) were solved numerically using a three-dimensional commercial CFD package, ANSYS 14.0 [23], which employs a finite volume method. The detail of this method is explained by Patankar [24]. The computational domain was meshed using hexagonal/wedge, tetrahedron and pyramid elements. A second-order upwind scheme was used to discretise the combined convection and diffusion terms in the momentum and energy equations and then the SIMPLE algorithm was employed to solve the coupled pressure-velocity fields in the equations.

The solution is assumed to converge when the normalised residuals of the continuity and momentum equation fall below 10^{-5} while that of the energy equation falls below 10^{-7}.

The convergence criterion for the peak temperature as the quantity monitored is:

$$\gamma = \left| \frac{(\Delta T_{max})_i - (\Delta T_{max})_{i-1}}{(\Delta T_{max})_i} \right| \le 0.01 \quad (25)$$

Where i is the mesh iteration index. The mesh is more refined as i increases and i-1 mesh was selected as the convergence criterion Equation (25) was satisfied.

The validation of the CFD code used was carried out by comparing the numerical results obtained using this code with the analytical results obtained from the investigation carried out in open literature [22]. The numerical results obtained in this study were also compared with the experimental results obtained by Wei *et al.* [13]. The results showed very good agreement with an average deviation of 2.4% as shown in Fig. 4a and 2.7% in Fig. 4b

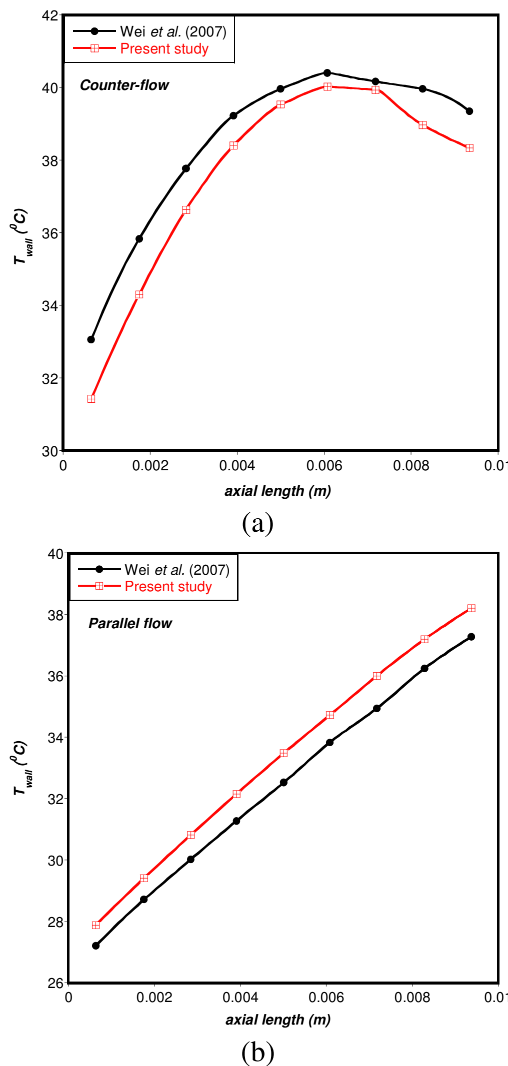

Fig. 4 Peak wall temperature along the length of a two-layer microchannel for parallel and counter flow of fluid

Table 1 shows the dimensions of the geometry used to carry out the grid refinement test [28] for the single microchannel heat sink while Table 2 shows the result of the grid refinement test for pressure drop of 30kPa.

Table 1: Dimensions of the microchannel heat sink for grid refinement test

t_1 (mm)	M-t_3 (mm)	t_3 (mm)	W_c (mm)	H_c (mm)	W (mm)	M (mm)	N (mm)
0.02	0.21	0.69	0.06	0.48	0.1	0.9	10

Table 2: Grid refinement test results

Number of cells	$\Delta T(K)$	$\left\lvert\frac{(\Delta T)_i-(\Delta T)_{i-1}}{\Delta(T)_i}\right\rvert$
18 458	14.3420	-
29 777	15.0306	0.0458
47 607	15.4470	0.0270
75 082	15.6063	0.0102
109 599	15.6545	0.0031

Grid refinement tests [28] were also carried out for the two-layer microchannel heat sinks at ΔP = 30kPa as shown in Table 4. Table 3 shows the dimensions of the geometry used for the grid refinement tests.

Table 3: Dimensions of the two-layer microchannel heat sink for grid refinement test

H_{c1}, H_{c2} (mm)	W_{c1}, W_{c2} (mm)	t_1, t_6 (mm)	M_1-t_3, M_2-t_5 (mm)	M_1, M_2 (mm)	W (mm)
0.250	0.06	0.02	0.10	0.45	0.10

Table 4: Grid refinement test results

Number of cells	$\Delta T(K)$	$\left\lvert\frac{(\Delta T)_i-(\Delta T)_{i-1}}{(\Delta T)_i}\right\rvert$
24 673	14.0978	-
39 969	14.2467	0.0105
59 374	14.1398	0.0076
83 866	14.2201	0.0056

OPTIMISATION PROCEDURE

In this study, the optimisation of the microchannel geometry is carried out using a goal-driven optimisation (GDO) tool in ANSYS 14.0 [22] whose main objective is to identify the relationship between the performance of a product and the design variables. It uses the response surface methodology (RSM) for its optimization process. The RSM uses a group of mathematical and statistical techniques to develop an adequate functional relationship between a response of interest and a number of input variables, which are explained further in literature with Equations [25, 26].

Once a model is created and parameters defined, a response surface is created. Based on the number of input parameters, a given number of solutions (design points) is required to build this response surface (an approximation of the response of the system). After inserting a response surface, the design space is defined by giving the minimum and maximum values to be considered for each input variable. The design of experiments (DOE) part of the response surface system creates the design space sampling and when updated, a response surface is created for each output parameter.

The GDO is an optimisation technique that finds design candidates from the response surfaces. The objective is set in the GDO and then the optimisation problem is solved. The accuracy of the response surface for the design candidates is checked by converting it to a design point, and thereafter, a full simulation is performed for that point to check the validity of the output parameters [23].

Numerical simulations and optimisation were carried out for a fixed total volume V of $0.9 mm^3$ with fixed length *N* of 10mm. The temperature of water pumped across the heat sinks was 20^0C and heat flux applied to the bottom wall was $1x10^6$ W/m^2. The design space for the response surface for the different solid volumes was defined as $54 \leq W_{c1}, W_{c2} \leq 66$ μm, $19 \leq t_1, t_6 \leq 29$ μm, $50 \leq M - t_3 \leq 60$ μm, $25 \leq M_1\text{-}t_3, M_2\text{-}t_5 \leq 30$ and $360 \leq H_{c1}, H_{c2} \leq 375$ μm. The optimised design point chosen was required to meet the manufacturing constraints. The range of pressure drop used throughout the simulations was between 10 and 60kPa. In the GDO, the objective function is to minimize the peak temperature in the heat sink and also minimize the temperature gradient on the heated base of the solid substrate based on the design space. For the micro pin-fins, the design space was defined as $30 \leq H_f \leq 160$ μm and $40 \leq D_f \leq 60$ μm for both the fixed and relaxed axial length while the pin-fin spacing *s* was fixed at 62.5μm with the micro pin-fins centrally placed in the microchannel.

DISCUSSION OF RESULTS

Figure 5 shows a comparison between the maximized thermal conductance of the different types of heat sinks considered in this study at different pressure drops and it was observed that as the pressure drop increases, the maximised thermal conductance increases for all the heat sinks considered in this study. At a constant solid volume *V* of $0.9mm^3$, fixed length *N* of 10mm and a pressure drop of 10kPa, the two-layer microchannel with parallel flow of fluid had the maximum thermal performance but as the pressure drop is increased up to 30kPa, the two-layer microchannel with counter-flow of fluid had the best thermal performance. When the pressure drop was further increased from 30kPa to 60kPa, the combined design of the single microchannel with three rows of micro pin fins had the best thermal performance. This result showed that the type of heat sink selected for best performance depends on the pressure drop.

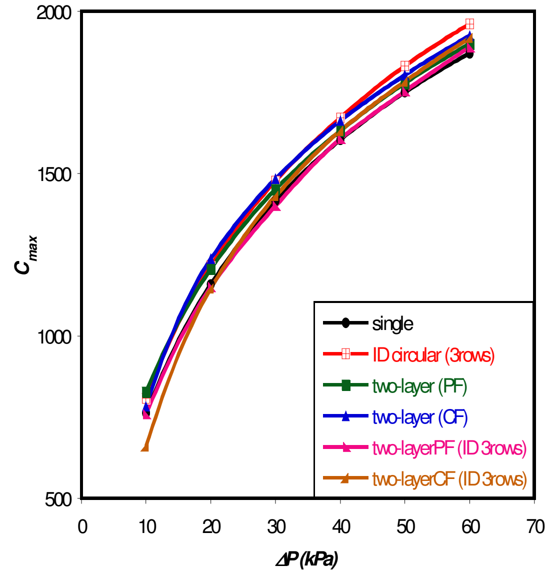

Figure 5 Maximised thermal conductance at different pressure drops

Figure 6 shows variations in temperature along the heated base of a solid substrate that is cooled with a single microchannel for different pressure drops. It is observed that the temperature gradient at pressure drop of 10kPa is very steep but as the pressure drop is increased there is a reduction in the thermal gradient. For a fixed axial length N of 10mm and constant solid volume V of $0.9mm^3$, The difference between the minimum and maximum temperature on the heated base is 16.03°C at a pressure drop of 10kPa. When the pressure drop was increased to 20kPa, the temperature difference was decreased by 42%. A further increase in the pressure drop to 60kPa further reduced the temperature difference by 50%.

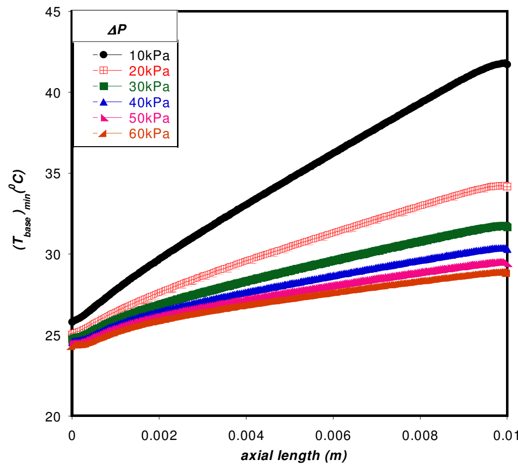

Figure 6 Temperature variations along the heated base of a solid substrate cooled by a single microchannel

Figure 7 shows the temperature variation on the heated base of a solid substrate cooled with a single microchannel with 3 rows of micro pin inserts. The volume is fixed with a fixed axial length of 10mm. The temperature difference on the heated base for pressure drop of 10kPa was 15.34˚C which gives about 4% improvement over the single microchannel with fixed axial length. There was 70% reduction in the temperature difference when the pressure drop was increased to 60kPa.

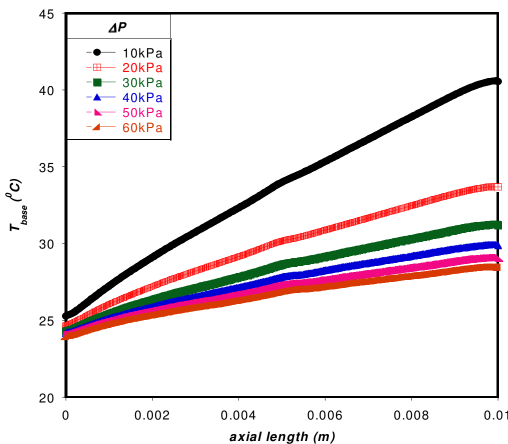

Figure 7 Temperature variations along the heated base of a solid substrate cooled by a single microchannel inserted with micro pin-fins

When a two-layer microchannel with parallel flow of fluid was used to cool the solid substrate of constant volume and fixed axial length, the temperature difference on the heated base decreased from 14.21˚C to 4.72˚C when the pressure drop was increased from 10kPa to 60kPa as shown in Figure 8.

The two-layer microchannel with counter-flow of fluid gave better results than that with parallel flow of fluid when the temperature variation in the heated base of the solid substrate is considered. The curve in the graph as we approach the centre of the axial length is as a result of the counter-flow of fluid which reduces the steep thermal gradient observed in the single microchannel and the two-layer microchannel with parallel flow of fluid. For a constant solid volume and fixed axial length, there was a decrease in temperature difference from 13.38˚C to 4.46˚C when pressure drop was increased from 10kPa to 60kPa. This is shown in Figure 9.

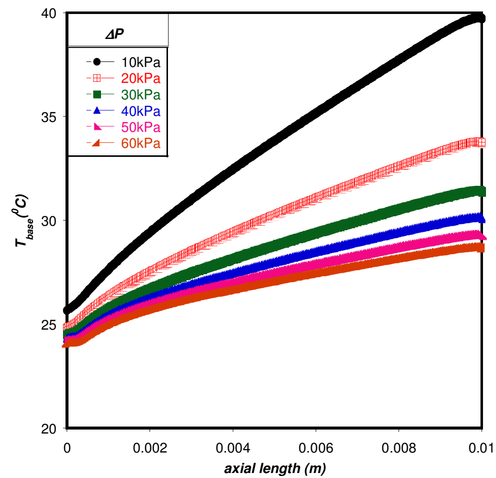

Figure 8 Temperature variations along the heated base of a solid substrate cooled by a two-layer microchannel with parallel flow of fluid

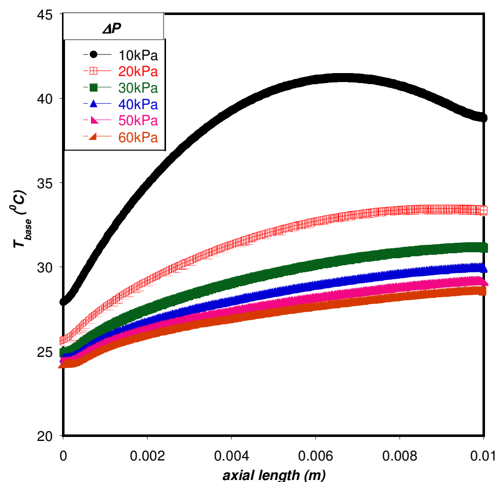

Figure 9 Temperature variations along the heated base of a solid substrate cooled by a two-layer microchannel with counter-flow of fluid

Figure 10 shows that the temperature difference on the heated base of the solid was further increased when the two-layer microchannel with parallel flow of fluid was inserted with three rows of micro pin fins. The temperature difference decreased from 16.57˚C to 5.34˚C when the pressure drop was increased from 10kPa to 60kPa.

The results of temperature difference of the heated base of the solid also increased when the two-layer microchannel with counter flow of fluid was inserted with micro pin fins. Figure 11 showed that the temperature difference decreased from 17.0°C to 5.02°C when the pressure drop increased form 10kPa to 60kPa. Figure 10 and 11 shows that the micro pin fins inserted in the centre of the microchannel reduces the temperature. This is shown by the dip observed in the graph at the mid-point of the axial length.

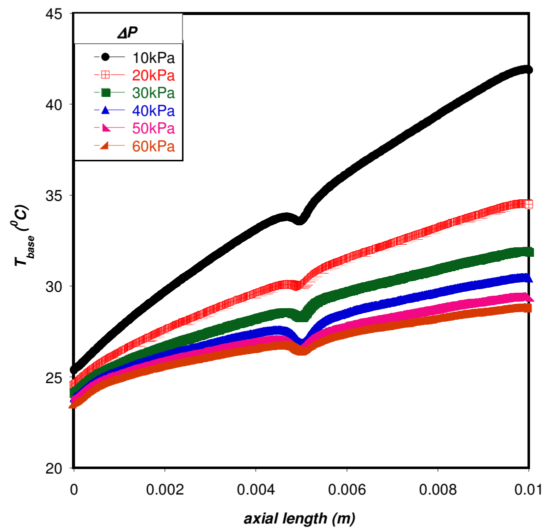

Figure 10 Temperature variations along the heated base of a solid substrate cooled by a two-layer microchannel with parallel flow of fluid inserted with 3 rows of micro pin-fins

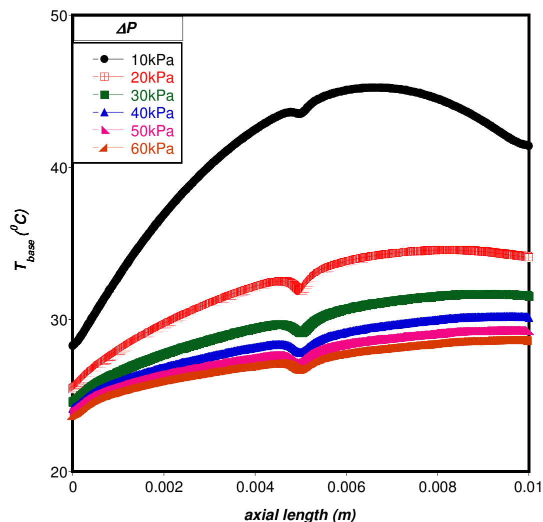

Figure 11 Temperature variations along the heated base of a solid substrate cooled by a two-layer microchannel with counter-flow of fluid inserted with 3 rows of micro pin-fins

Figure 12 shows a comparison between the temperatures differences on the heated base of the solid substrate cooled by the different heat sink considered in this study. Results showed that for a fixed axial length and constant solid volume, the two-layer microchannel with counter flow of fluid had the best result for all the pressure drops considered.

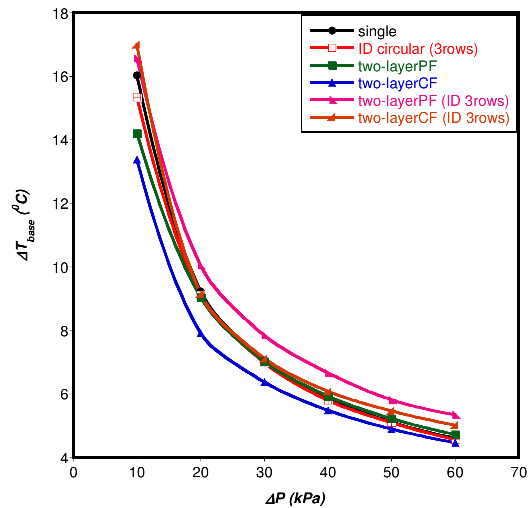

Figure 12 Comparison between the temperature difference on the heated base of the solid substrate cooled by the different heat sink

CONCLUSIONS

In this study, three-dimensional numerical study was carried out to investigate the temperature variation on the heated base of a solid substrate cooled using six different types of heat sinks. A high temperature difference on the heated base indicates a high thermal gradient which leads to thermal stresses. The heat sink that gave a maximum thermal conductance and lowest temperature difference on the heated base was chosen as the best heat sink design. The design parameters of the different heat sinks considered in this study have been optimised based on maximised thermal conductance.

For a fixed solid volume V of 0.9mm^3 and fixed axial length N of 10mm, results showed that for maximum thermal conductance, the best heat sink design depends on the pressure drop. At the lowest pressure drop of 10kPa considered in this study, the two-layer microchannel with parallel flow arrangement gave the maximum thermal conductance. When the pressure drop was increased up to 30kPa, the two-layer microchannel with counter flow arrangement gave the maximum thermal conductance. Further increasing the pressure drop up to the maximum of 60kPa considered in this study, the single microchannel with three rows of micro pin-fin inserts gave maximum thermal conductance.

When temperature difference on the heated base was studied, the two-layer microchannel with counter flow arrangement gave the lowest

temperature difference for all the pressure drops considered in this study.

These results showed that at pressure drops of 20 and 30kPa, the two-layer microchannel with counter flow of fluid is the best design in maximising thermal conductance and minimising the temperature variation on the heated base.

ACKNOWLEDGEMENTS

The funding obtained from NRF, TESP, University of Stellenbosch/ University of Pretoria, SANERI/SANEDI, CSIR, EEDSM Hub and NAC is acknowledged and duly appreciate.

REFERENCES

[1] Tuckerman D.B., and Pease R.F.W., High Performance heat sinking for VLSI, *IEEE Electronic Device Letters EDL-2*, 1981, pp. 126-129

[2] Knight R.W., Hall D.J., Goodling J.S., and Jaeger R.C., Heat Sink Optimization with Application to Micro-channels, *IEEE Transactions of Components, Hybrids and Manufacturing Technology*, 15, 1992, pp. 832-842

[3] Murakami Y., and Mikic B.B, Parametric Optimization of Multi-channeled Heat Sinks for VLSI Chip Cooling, *IEEE Transactions on Components and Packaging Technologies*, 24, 2001, pp. 2-9

[4] Upadhye H.R., and Kandlikar S.G., Optimization of Micro-channel Geometry for Direct Chip Cooling Using Single Phase Heat Transfer, *ASME Conference on Micro-channels and Mini-channels*, 2004, Rochester, New York, USA

[5] Ryu J.H., Choi D.H., and S.J. Kim S.J., Numerical optimization of the thermal performance of a micro-channel heat sink, *International Journal of Heat and Mass Transfer,* 45, 2002, pp. 2823-2827

[6] Ryu J.H., Choi D.H., and Kim S.J., Three-dimensional numerical optimization of a manifold micro-channel heat sink, *International Journal of Heat and Mass Transfer*, 46, 2003, pp. 1553-1562

[7] Muller N., and Frechette L.G., Optimization and Design Guidelines for High Flux Micro-Channel Heat Sinks for Liquid and Gaseous Single-Phase Flow, *Inter Society Conference on Thermal Phenomena*, 2002, pp. 449-456

[8] Li J., and Peterson G.P., Geometric Optimization of a Micro Heat Sink with Liquid Flow, *IEEE Transactions on Component and Packaging Technologies*, 29, 2006, pp. 145-154

[9] Li J., and Peterson G.P., 3-Dimensional numerical optimization of silicon-based high performance parallel micro-channel heat sink with liquid flow, *International Journal of Heat and Mass Transfer*, 50, 2007, pp. 2895-2904

[10] Husain A., and Kim K., Shape Optimization of Micro-Channel Heat Sink for Micro-Electronic Cooling, *IEEE Transactions on Components and Packaging Technologies*, 31, 2008, pp. 322-330

[11] Bello-Ochende T., Meyer J.P., and Ighalo F.U., Combined numerical optimization and constructal theory for the design of micro-channel heat sinks, *Numerical Heat Transfer, Part A*, 58, 2010, pp. 882-899

[12] Bello-Ochende T., Liebenberg L., and Meyer J.P., Constructal cooling channels for micro-channel heat sinks, *International Journal of Heat and Mass Transfer*, 50, 2007, pp. 4141-4150.

[13] Wei X., Joshi Y., and Patterson M.K., Experimental and numerical study of stacked micro-channel heat sink for liquid cooling of microelectronic devices, *Journal of Heat Transfer*, 129, 2007, pp. 1432-1444

[14] Wei X., Stacked micro-channel heat sinks for liquid cooling of microelectronic devices, PhD Thesis, 2004

[15] Patterson M.K., Wei X., Joshi Y., and Prasher R., Numerical study of conjugate heat transfer in stacked micro-channels, *Inter Society Conference on Thermal Phenomena*, 2004, pp. 372-380

[16] Wei X., and Joshi Y., Optimization study of stacked microchannel heat sinks for micro-electronic cooling, *IEEE Transactions on Components and Packaging Technologies*, 26, 2003, pp. 55-61

[17] Wei X., and Joshi Y., Stacked micro-channel heat sinks for liquid cooling of microelectronic components, *Journal of Electronic Packaging*, 126, 2004, pp. 60-66

[18] Jeevan K., Azid I.A., and Seetharamu K.N., Optimization of double layer counter flow (DLCF) micro-channel heat sink used for cooling chips directly, *Electronics Packaging Technology Conference*., 2004, pp. 553-558

[19] Jeevan K., Quadir G.A., Seetharamu K.N., Azid I.A., and Zainal Z.A., Optimization of thermal resistance of stacked micro-channel using genetic algorithms, *International Journal of Numerical Methods in Heat and Fluid Flow*, 15, 2005, pp. 27-42

[20] Chong S.H., Ooi K.T., and Wong T.N., Optimization of single and double layer counter flow micro-channel heat sinks, *Applied Thermal Engineering*, 22, 2002, pp. 1569-1585

[21] Hung T., Yan W., and Li W., Analysis of heat transfer characteristics of double-layered microchannel heat sink, *International Journal of Heat and Mass Transfer*, 55, 2012 pp. 3090-3099

[22] Adewumi O.O., Bello-Ochende T., and Meyer J.P., Constructal design of combined microchannel and micro pin fins for electronic cooling, *International Journal of Heat and Mass Transfer*, 66, 2013, pp. 315-323
[23] ANSYS FLUENT *14.0 User's Guide Documentation*, 2011
[24] Pantakar S.V., *Numerical Heat Transfer and Fluid Flow*, Hemisphere Publishing Corp., 1980
[25] Khuri A.I., and Mukhopadhyay S., Response surface methodology, *Advanced Review*, 2, 2010, pp. 128-149
[26] Myers R.H., and Montgomery D.C., *Response surface methodology: Process and product optimization using designed experiments*, Wiley, New York, 2002
[27] Ighalo F.U., Optimisation of microchannels and micropin-fin heat sinks with computational fluid dynamics in combination with a mathematical optimisation algorithm. *MSc Thesis, Department of Mechanical and Aeronautical Engineering, University of Pretoria*, 2010
[28] LEAP support team 2012, Tips & Tricks: Convergence and mesh independence study, viewed June 2012, http://www.computationalfluiddynamics.com.au/convergence-and-mesh-independent-study/.